This is a repository copy of *Potential to measure quantum effects in recent all-optical radiation reaction experiments*.

White Rose Research Online URL for this paper:
https://eprints.whiterose.ac.uk/158814/

Version: Accepted Version

Proceedings Paper:

ABSTRACT

The construction of 10 PW class laser facilities with unprecedented intensities has emphasised the need for a thorough understanding of the radiation reaction process. We describe simulations for a recent all-optical colliding pulse experiment, where a GeV scale electron bunch produced by a laser wakefield accelerator interacted with a counter-propagating laser pulse. In the rest frame of the electron bunch, the electric field of the laser pulse is increased by several orders of magnitude, approaching the Schwinger field and leading to substantial variation from the classical Landau-Lifshitz model. Our simulations show how the final electron and photon spectra may allow us to differentiate between stochastic and semi-classical models of radiation reaction, even when there is significant shot-to-shot variation in the experimental parameters. In particular, constraints are placed on the maximum energy spread and shot-to-shot variation permissible if a stochastic model is to be proven with confidence.

Potential to measure quantum effects in recent all-optical radiation reaction experiments

C. Arran[1], J. M. Cole[2], E. Gerstmayr[2], T. G. Blackburn[3], S. P. D. Mangles[2], and C. P. Ridgers[1]

[1]York Plasma Institute, University of York, York, United Kingdom
[2]The John Adams Institute for Accelerator Science, Imperial College London, London, United Kingdom
[3]Department of Physics, Chalmers University of Technology, Gothenburg, Sweden

1. INTRODUCTION

In the years ahead, a number of new laser facilities will reach unprecedented ultra-high intensities. Apollon 10 PW (1) and ELI (2; 3) will access new physics regimes at laser intensities of up to $10^{22-24}\,\mathrm{Wcm^{-2}}$, where strong-field QED processes will strongly modify the laser-plasma dynamics. In one of these processes, radiation reaction, electrons emitting synchrotron radiation in the presence of strong electro-magnetic fields lose energy and recoil; as the field intensity increases this energy loss approaches 100% of the initial electron energy and the classical model of radiation reaction breaks down. This strongly affects studies of inverse Compton scattering (4; 5) and ion acceleration (6; 7; 8; 9), which are both priorities for the next generation of laser facilities.

Modelling the process of radiation reaction with strong-field QED is however difficult, requiring knowledge of the final asymptotic free states and the solutions are normally restricted to limited cases, such as a plane wave. Instead, a set of tractable models have been developed, in which the synchrotron emission spectrum is modified as described by Sokolov *et al.* (10). The electron energy loss can then be described either using continuous emission in a semi-classical model, or by a sequence of discrete and stochastic emission events in a 'quantum' model, which can be incorporated into Particle-In-Cell (PIC) codes using a Monte-Carlo algorithm (e.g. (11)). However, the Sokolov model assumes that photon emission is significantly faster than changes in the field, in the locally constant crossed field approximation; this is only accurate for field strengths $a_0 = eE_L/m_e\omega c \gg 1$ (12), and then only for high energy photons. Recently, computational work has demonstrated that this is a sufficiently good approximation for describing the dynamics of radiation reaction in the strong-field regime (13) but as of yet experimental evidence has been elusive.

Two recent experiments (14; 15) have attempted to test these models with all-optical set-ups similar to those envisaged for ELI-NP, but with peak laser intensities of $\sim 10^{21}\,\mathrm{Wcm^{-2}}$ using existing laser facilities. In these experiments, high energy electrons are accelerated by a laser-driven plasma wakefield (16; 17; 18) to energies on the scale of GeV, with $\gamma \approx 1000 - 2000$. A second counter-propagating laser pulse is brought to a high intensity focus near the end of the plasma such that the electric field experienced in the rest frame of the electron, $E_L' = \gamma E_L \sim 10^{17}\,\mathrm{V/m}$, approaches the Schwinger limit, $E_s = 1.32 \times 10^{18}\,\mathrm{V/m}$. The dimensionless and Lorentz invariant parameter $\chi_e = E_L'/E_s$ describes the divergence from the classical predictions; when χ_e approaches 1 the classical synchrotron spectrum would require producing photons with energies greater than the initial energy of the electron. Both experiments measured strong evidence for radiation reaction and demonstrated better agreement with the quantum corrected models than with the classical Landau-Lifschitz model (19), even though χ_e was significantly less than 1.

There was, however, insufficient evidence to conclude whether stochastic emission effects were present, and Poder *et al.*(15) measured slightly better agreement with the semi-classical model, leaving significant uncertainty (20), particularly about the use of the locally constant crossed field approximation at low a_0. One of the main problems was measuring a large number of shots where collisions were definitely present, given significant shot-to-shot variation in the timing and pointing of the two laser beams. Experiments attempting to measure more successful collisions at higher values of χ_e are therefore on-going in attempts to resolve the uncertainty.

This paper describes a potential way to measure the effect of quantum stochastic processes in all-optical radiation reaction experiments, and places constraints on the experimental parameters required. The aim is to

conclude with confidence, using as few collisions as possible, that one or the other model is more correct under these conditions. In order to do this, shot-to-shot variations in the experimental parameters must also be strictly controlled, to tolerances described in this paper. Whereas a previous paper by the authors (21) has explored the parameter spaces of electron energy and laser intensity required, this paper aims to show a clear constraint on the maximum electron energy spread permitted if stochastic effects are to be measured.

2. MONTE-CARLO SIMULATED EXPERIMENTS

By running Monte-Carlo simulated experiments it was possible to calculate the expected measurements for each of the possible models while taking account of experimental errors and uncertainties. For each of 10,000 simulated shots, a new electron distribution was formed, with its mean energy and energy spread both chosen at random from within the specified shot-to-shot variation. 10,000 electrons were sampled from this distribution and collided with a laser intensity again drawn at random from within the specified experimental error. For each electron the final electron energy and the spectrum of photons produced were inferred from mono-energetic simulations conducted with the PIC code EPOCH (22), for each of the classical, semi-classical and quantum models. The final electron and photon spectra were then fitted to make simulated measurements of the mean final electron energy $\langle \varepsilon_f \rangle$, the final electron energy spread σ_{ε_f}, and the critical energy of emitted photons $\varepsilon_{\mathrm{crit}}$ for each shot. These were combined by a Gaussian kernel density estimate to approximate the joint probability distribution function.

The first conditions simulated were those described by Cole *et al.*(14), in order to verify the Monte-Carlo simulations. The mean electron energy was $\langle \varepsilon_i \rangle = (550 \pm 20)\,\mathrm{MeV}$, while the energy spread was $\sigma_{\varepsilon_i} = 250\,\mathrm{MeV}$. The laser intensity was described by $a_0 = 11 \pm 3$. The surfaces shown in Fig. 1 are the contours of the probability distribution function, inside which are contained the most likely possible measurements of each of the three final variables. Shots which encountered a lower a_0 lead to higher final electron energies, lower photon energies, and higher electron energy spread. The breadth of the probability distributions reflect the large errors on both the laser a_0 and on the initial electron distributions.

It is clear from these results that the classical model predicts significantly higher photon energies than after the quantum correction, allowing this model to be distinguished from the other two by measuring a combination of the mean final electron energy $\langle \varepsilon_f \rangle$ and the photon critical energy $\varepsilon_{\mathrm{crit}}$. The deterministic semi-classical model and the stochastic quantum model predict very similar results, however, and a measurement of the mean final energy will struggle to distinguish them. Measuring the final electron energy spread, however, increasingly separates the three models at higher a_0; in the stochastic model the energy spread reduces substantially slower due to stochastic broadening, allowing measurements of the electron spectrum alone to differentiate between models.

3. MODEL OVERLAP

It is possible to quantify the possibility of distinguishing between models by defining a model overlap Ω, which is 0 if the models have entirely different predictions, and 1 if the predictions are identical. Assuming that two given models are both equally likely and that all measurements are equally likely in the region of interest, the probability of misidentifying one model as true, given that the other one is in fact true, is then given by:

$$P(A|B) = P(B|A) = \Omega \equiv \frac{\int P(\mathbf{x}|A) \cdot P(\mathbf{x}|B) \mathrm{d}V_{\mathbf{x}}}{\sqrt{\int P(\mathbf{x}|A)^2 \mathrm{d}V_{\mathbf{x}} \int P(\mathbf{x}|B)^2 \mathrm{d}V_{\mathbf{x}}}}, \tag{1}$$

where $\mathbf{x}$ is a vector of the possible measurements (in our case a 3-vector for $\langle \varepsilon_f \rangle$, $\varepsilon_{\mathrm{crit}}$, and σ_{ε_f}), $P(\mathbf{x}|A)$ is the likelihood of measuring $\mathbf{x}$, given that model A is true under the experimental conditions, and the integrations are performed over all the domain of all possible measurements in the region of interest.

If we wish to reduce the probability of misidentifying a model we can take multiple shots; if we take N independent and identically distributed measurements the probability of falsely concluding that one of the models is true becomes: $p = \Omega^N$. Conversely, if we wish to conclude with a confidence $(1 - p)$ that one model is better
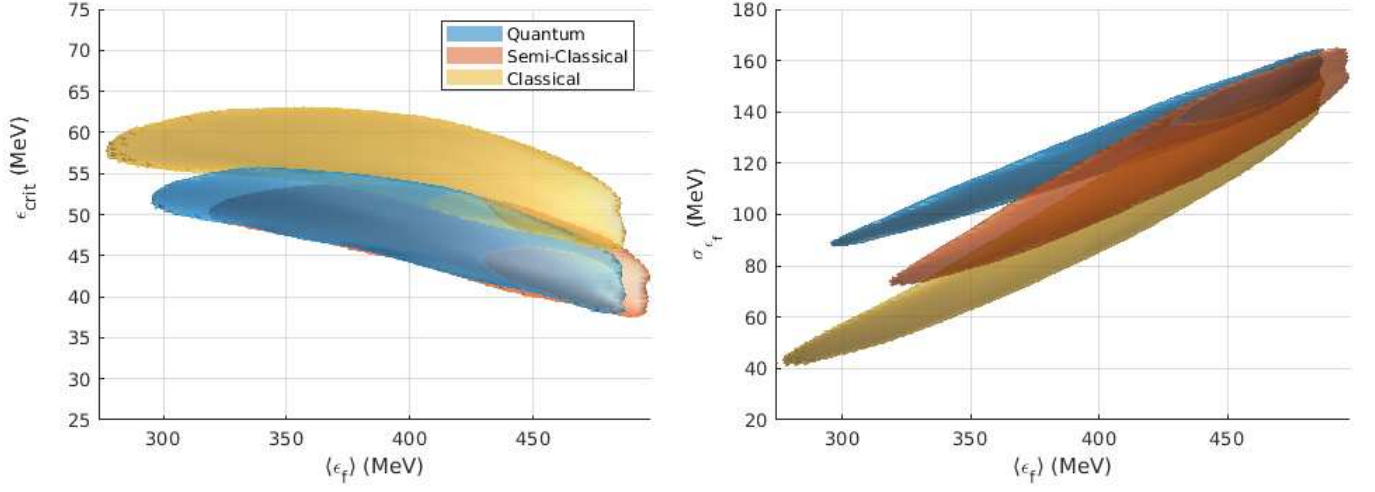
Figure 1. The most likely measurements of $\langle \varepsilon_f \rangle$, $\varepsilon_{\mathrm{crit}}$, and σ_{ε_f}, given an initial electron beam with a peak energy of (550 ± 20) MeV and an energy spread of 250 MeV and a laser intensity of $a_0 = 11 \pm 3$. The 1σ contours are shown of the 3-dimensional joint probability distribution function, within which 68% of simulated experiments measured these results, assuming each of the classical (yellow), semi-classical (red), and quantum (blue) models. The two plots are two views of the same three dimensional surfaces.
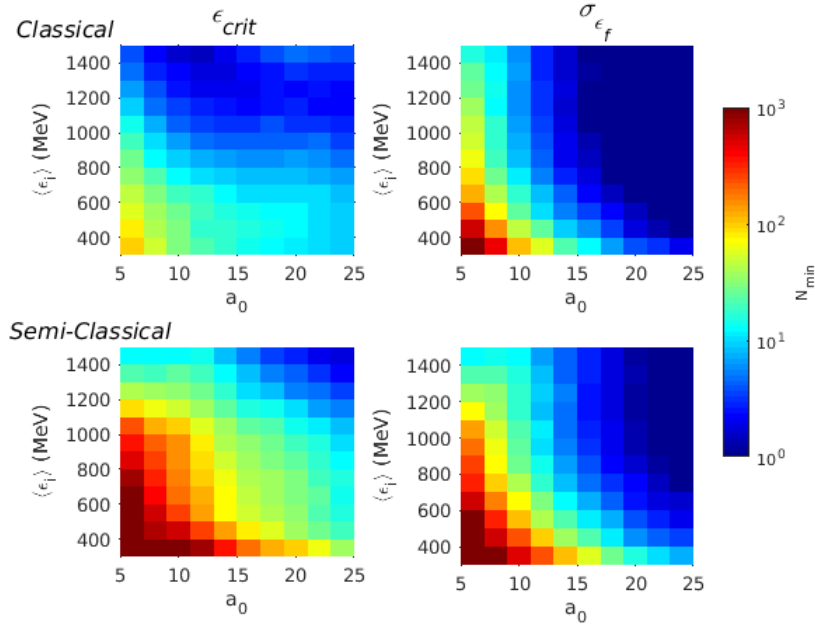

Figure 2. The number of shots required to distinguish between models with a confidence of 3σ, at a range of initial electron energies and laser intensities, using measurements of (left) $\langle \varepsilon_f \rangle$ and $\varepsilon_{\mathrm{crit}}$ and (right) $\langle \varepsilon_f \rangle$ and σ_{ε_f}. The chosen models for comparison were (top) quantum and classical, and (bottom) quantum and semi-classical. The initial electron energy spread was 50% of the initial mean electron energy, the shot-to-shot variation on the a_0 was ± 3, and the relative variation on both the mean electron energy and the energy spread was 10%.

than another, we require $N_{\min} \geq \log(p)/\log(\Omega)$ shots. As $\Omega \to 1$, $N_{\min} \to \infty$, making it impossible to distinguish between two models.

We ran simulated experiments under a range of conditions in order to find the number of shots required to distinguish between the Monte-Carlo quantum model and each of the two alternatives: the classical Landau-Lifschitz model, and the quantum-corrected semi-classical model. In both cases, rather than calculating the full 3-dimensional joint distribution function, two 2-dimensional distribution functions were calculated, for measurements of $\langle \varepsilon_f \rangle$ and $\varepsilon_{\mathrm{crit}}$, and for measurements of $\langle \varepsilon_f \rangle$ and σ_{ε_f}; these are essentially averages of the 3-dimensional distribution function taken over one of the dimensions. Throughout, the parameters were chosen for broad electron energy distributions, with initial energy spread 50% of the mean electron energy. The relative shot-to-shot variation on both mean electron energy and on energy spread were chosen as 10% while the a_0 varied with an error of ± 3. Other simulated experiments not described here demonstrated that the effect of errors on a_0 are fairly minimal when calculating model overlap.

We can see in Fig. 2 that when distinguishing between the classical and quantum models, measurements of $\varepsilon_{\mathrm{crit}}$ as made by Cole *et al.*(14) are successful, with only tens of shots or fewer required to establish a $1-p = 99.7\%$ confidence in either one model or the other being correct. As expected, distinguishing models becomes easier when radiation reaction effects are more prominent at higher laser intensities and at higher initial electron energies, with fewer than 10 shots required when the electron energy is greater than around $1\,\mathrm{GeV}$. The saturation of $\varepsilon_{\mathrm{crit}}$ with a_0 also implies that the benefit of increasing laser intensity is smaller than the benefit of increasing electron energy.

When the semi-classical model is considered, however, it becomes much more difficult to demonstrate that stochastic effects are or are not present by using measurements of $\varepsilon_{\mathrm{crit}}$; hundreds of shots or more are required when the laser intensity is less than $a_0 \approx 15$ and the initial electron energy is around $1\,\mathrm{GeV}$ or less. Another measurement is required to distinguish between the quantum and semi-classical models with confidence.

Measuring the change in electron energy spread is substantially more successful at determining between quantum and semi-classical models; for values of $a_0 \geq 15$ the models can normally be distinguished in under 10 shots, and at higher laser intensities and electron energies only a single shot would be required. At these higher laser intensities, a measurement of electron energy spread is also more successful at distinguishing between quantum and classical models than a measurement of the photon critical energy.

Depending on which models are in question and on the experimental parameters, different measurements are the best to make. For distinguishing quantum and semi-classical models, a measurement of the electron energy spread is generally significantly more successful. For distinguishing quantum and classical models, however, a measurement of the photon critical energy is more successful at lower laser intensities, and a measurement of the electron energy spread is more effective at laser intensities with $a_0 \geq 15$.

4. REQUIRED PARAMETERS

Using parameter scans as above, it is possible to place restrictions on the energy spread allowable to distinguish in a limited number of shots between quantum and semi-classical models of radiation reaction. Simulated experiments were run at $a_0 = 10$ and $a_0 = 20$ for a range of electron energies and at a range of electron energy spreads, where the shot-to-shot variation in a_0 was ± 3, and the relative shot-to-shot variation in both $\langle E_i \rangle$ and σ_{E_i} was 20%. From the resulting 2-dimensional surfaces (an example is shown in Fig. 3a), the contour for $N_{\min} = 10$ given $p = 0.003$ was found, determining the level required to establish a 99.7% in one model rather than another in 10 shots or fewer; this is a reasonable threshold for a given radiation reaction experiment to be successful in distinguishing between quantum and semi-classical models of radiation reaction. The contours are shown in Fig. 3b).

Fig 3 demonstrates, firstly, that when the electron energy is high, a larger energy spread is permitted for the effects of stochastic broadening to be observed. This effect is described in refs (23; 24), but whereas they describe a requirement $\sigma_{\varepsilon_i}/\langle \varepsilon_i \rangle \lesssim 0.77\eta^{0.5}$ for stochastic broadening to dominate over radiative cooling, we observe that the effect of stochastic broadening becomes clear even at significantly higher energy spreads. At $a_0 = 10$ and $\langle E_i \rangle > 1\,\mathrm{GeV}$, the energy spread can be $\sigma_{\varepsilon_i}/\langle \varepsilon_i \rangle \approx 30\%$ and the effect of stochastic broadening will still be
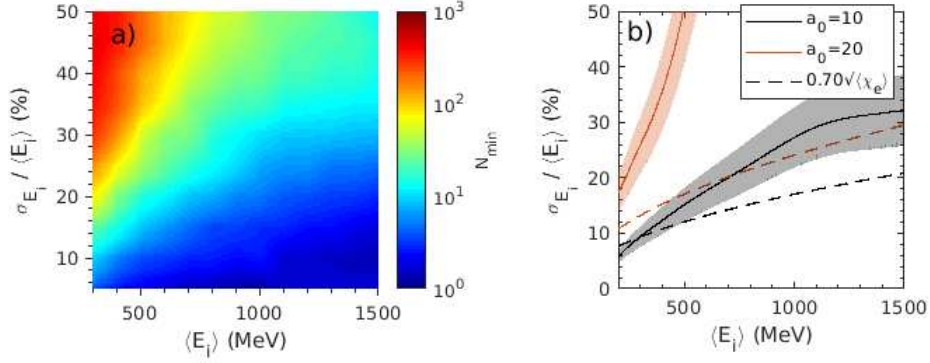
Figure 3. a) Colour map of the number of shots required to distinguish between quantum and semi-classical models of radiation reaction at $a_0 = 10 \pm 3$. Relative shot-to-shot variations in $\langle E_i \rangle$ and σ_{E_i} are 20%. For illustrative purposes the surface is interpolated between discrete simulations. b) The estimated maximum allowable energy spread at $a_0 = 10$ (black) and $a_0 = 20$ (red), in order to measure with 99.7% confidence the effect of stochastic broadening using 10 shots or fewer. Allowable shot-to-shot variation in σ_{E_i} is shown by the shaded areas and the results of Monte-Carlo simulated experiments are compared to the analytic threshold for stochastic broadening to dominate momentarily over cooling (dashed lines).

measurable; that is, although the energy distribution does not become any broader, it narrows by significantly less than predicted by a deterministic model.

Next, when the laser intensity is high, with $a_0 = 20$, even very large energy spreads will not prevent stochastic broadening from being measured. In this regime, the rate of cooling in the semi-classical model is very rapid, and if the semi-classical model is a good description then the electron energy spectrum will become extremely narrow, regardless of the initial energy spread. Both refs. (15) and (14) measured electron energy distributions with extremely high energy spreads, but while this is makes measuring stochastic effects very difficult at lower laser intensities, it is no longer a barrier at very high laser intensites.

5. CONCLUSIONS

We have described how different possible measurements of radiation reaction experiments can enable the measurement of quantum effects, both through the change in the emission rates and the resulting photon spectrum and the appearance of stochastic effects and the consequent broadening of the electron energy spread compared to a deterministic model. The possible measurements were described by a joint probability distribution function assuming each of a classical, Landau-Lifschitz, model, a semi-classical model with continuous emission but adjusted emission rates, and a quantum model with both adjusted emission rates and random stochastic emission. These were calculated through Monte-Carlo simulated experiments, allowing us to conduct parameter scans over a range of experimental parameters.

In turn, the joint distribution functions allowed us to calculate the model overlap under different conditions and to estimate the number of shots required before a radiation reaction experiment could successfully distinguish between two different models. We used this to show that whereas measuring the photon critical energy is effective at distinguishing between quantum and classical models at lower laser intensities, $a_0 \lesssim 15$, a measurement of the final electron energy spread is more effective at distinguishing between the models at higher laser intensities, and is much better at showing evidence for stochastic effects.

We then used the simulated experiments to place restrictions on the initial energy spread required to measure evidence for stochastic effects. Whereas a very small energy spread is required for the electron spectrum to become broader (on the scale of 10% at the experimental parameters described), it is possible to confidently conclude the presence of stochastic broadening even at much higher initial electron energy spreads.

ACKNOWLEDGMENTS

This work is strongly related to another paper, which has been submitted for publication in Plasma Physics and Controlled Fusion. The simulated experiments are conducted in the same manner, using the same mono-energetic Particle-in-Cell simulations. However, a different approach is taken to exploring the parameter space and different results are presented.

References

[1] J. Zou, C. Le Blanc, D. Papadopoulos, G. Chériaux, P. Georges, G. Mennerat, F. Druon, L. Lecherbourg, A. Pellegrina, P. Ramirez, F. Giambruno, A. Fréneaux, F. Leconte, D. Badarau, J. Boudenne, D. Fournet, T. Valloton, J. Paillard, J. Veray, M. Pina, P. Monot, J. Chambaret, P. Martin, F. Mathieu, P. Audebert, and F. Amiranoff, "Design and current progress of the Apollon 10 PW project," *High Power Laser Science and Engineering* **3**, 2015.

[2] S. Weber, S. Bechet, S. Borneis, L. Brabec, M. Bučka, E. Chacon-Golcher, M. Ciappina, M. DeMarco, A. Fajstavr, K. Falk, E. R. Garcia, J. Grosz, Y. J. Gu, J. C. Hernandez, M. Holec, P. Janečka, M. Jantač, M. Jirka, H. Kadlecova, D. Khikhlukha, O. Klimo, G. Korn, D. Kramer, D. Kumar, T. Lastovička, P. Lutoslawski, L. Morejon, V. Olšovcová, M. Rajdl, O. Renner, B. Rus, S. Singh, M. Šmid, M. Sokol, R. Versaci, R. Vrána, M. Vranic, J. Vyskočil, A. Wolf, and Q. Yu, "P3: An installation for high-energy density plasma physics and ultra-high intensity laser–matter interaction at ELI-Beamlines," *Matter and Radiation at Extremes* **2**, pp. 149–176, July 2017.

[3] S. Gales, K. A. Tanaka, D. L. Balabanski, F. Negoita, D. Stutman, O. Tesileanu, C. A. Ur, D. Ursescu, I. Andrei, S. Ataman, M. O. Cernaianu, L. D'Alessi, I. Dancus, B. Diaconescu, N. Djourelov, D. Filipescu, P. Ghenuche, D. G. Ghita, C. Matei, K. Seto, M. Zeng, and N. V. Zamfir, "The extreme light infrastructure—nuclear physics (ELI-NP) facility: New horizons in physics with 10 PW ultra-intense lasers and 20 MeV brilliant gamma beams," *Reports on Progress in Physics* **81**, p. 094301, Sept. 2018.

[4] N. D. Powers, I. Ghebregziabher, G. Golovin, C. Liu, S. Chen, S. Banerjee, J. Zhang, and D. P. Umstadter, "Quasi-monoenergetic and tunable X-rays from a laser-driven Compton light source," *Nat. Photonics* **8**, pp. 28–31, Nov. 2013.

[5] H. E. Tsai, X. Wang, J. Shaw, A. V. Arefiev, Z. Li, X. Zhang, R. Zgadzaj, W. Henderson, V. Khudik, G. Shvets, and M. C. Downer, "Compact tunable Compton x-ray source from laser wakefield accelerator and plasma mirror," *Phys. Plasmas* **22**(2), p. 023106, 2016.

[6] M. Tamburini, F. Pegoraro, A. D. Piazza, C. H. Keitel, and A. Macchi, "Radiation reaction effects on radiation pressure acceleration," *New J. Phys.* **12**(12), p. 123005, 2010.

[7] P. Zhang, C. P. Ridgers, and A. G. R. Thomas, "The effect of nonlinear quantum electrodynamics on relativistic transparency and laser absorption in ultra-relativistic plasmas," *New J. Phys.* **17**(4), p. 043051, 2015.

[8] W.-M. Wang, P. Gibbon, Z.-M. Sheng, Y.-T. Li, and J. Zhang, "Laser opacity in underdense preplasma of solid targets due to quantum electrodynamics effects," *Phys. Rev. E* **96**, p. 013201, July 2017.

[9] M. J. Duff, R. Capdessus, D. D. Sorbo, C. P. Ridgers, M. King, and P. McKenna, "Modelling the effects of the radiation reaction force on the interaction of thin foils with ultra-intense laser fields," *Plasma Physics and Controlled Fusion* **60**, p. 064006, June 2018.

[10] I. V. Sokolov, J. A. Nees, V. P. Yanovsky, N. M. Naumova, and G. A. Mourou, "Emission and its back-reaction accompanying electron motion in relativistically strong and QED-strong pulsed laser fields," *Phys. Rev. E* **81**, p. 036412, Mar. 2010.

[11] C. Ridgers, J. Kirk, R. Duclous, T. Blackburn, C. Brady, K. Bennett, T. Arber, and A. Bell, "Modelling gamma-ray photon emission and pair production in high-intensity laser–matter interactions," *Journal of Computational Physics* **260**, pp. 273–285, Mar. 2014.

[12] V. I. Ritus, "Quantum effects of the interaction of elementary particles with an intense electromagnetic field," *J. Russ. Laser Res.* **6**, pp. 497–617, Sept. 1985.

[13] T. G. Blackburn, D. Seipt, S. S. Bulanov, and M. Marklund, "Benchmarking semiclassical approaches to strong-field QED: Nonlinear Compton scattering in intense laser pulses," *Physics of Plasmas* **25**, p. 083108, Aug. 2018.

[14] J. M. Cole, K. T. Behm, E. Gerstmayr, T. G. Blackburn, J. C. Wood, C. D. Baird, M. J. Duff, C. Harvey, A. Ilderton, A. S. Joglekar, K. Krushelnick, S. Kuschel, M. Marklund, P. McKenna, C. D. Murphy, K. Poder, C. P. Ridgers, G. M. Samarin, G. Sarri, D. R. Symes, A. G. R. Thomas, J. Warwick, M. Zepf, Z. Najmudin, and S. P. D. Mangles, "Experimental Evidence of Radiation Reaction in the Collision of a High-Intensity Laser Pulse with a Laser-Wakefield Accelerated Electron Beam," *Phys. Rev. X* **8**(1), pp. 8–13, 2018.

[15] K. Poder, M. Tamburini, G. Sarri, A. Di Piazza, S. Kuschel, C. D. Baird, K. Behm, S. Bohlen, J. M. Cole, D. J. Corvan, M. Duff, E. Gerstmayr, C. H. Keitel, K. Krushelnick, S. P. D. Mangles, P. McKenna, C. D. Murphy, Z. Najmudin, C. P. Ridgers, G. M. Samarin, D. R. Symes, A. G. R. Thomas, J. Warwick, and M. Zepf, "Experimental Signatures of the Quantum Nature of Radiation Reaction in the Field of an Ultraintense Laser," *Physical Review X* **8**, July 2018.

[16] S. P. D. Mangles, C. D. Murphy, and Z. Najmudin, "Monoenergetic beams of relativistic electrons from intense laser-plasma interactions," *Nature* **431**, pp. 535–538, 2004.

[17] J. Faure, Y. Glinec, A. Pukhov, S. Kiselev, S. Gordienko, E. Lefebvre, J.-P. Rousseau, F. Burgy, and V. Malka, "A laser–plasma accelerator producing monoenergetic electron beams," *Nature* **431**, pp. 541–544, Sept. 2004.

[18] C. G. R. Geddes, C. S. Toth, J. Van Tilborg, E. Esarey, C. B. Schroeder, D. Bruhwiler, C. Nieter, J. Cary, and W. P. Leemans, "High-quality electron beams from a laser wakefield accelerator using plasma-channel guiding.," *Nature* **431**(7008), pp. 538–541, 2004.

[19] L. D. Landau and E. M. Lifshitz, *The Classical Theory of Fields*, vol. 2, Pergamon Press, 3 ed., 1971.

[20] A. Macchi, "Intense Laser Sheds Light on Radiation Reaction," *APS Physics* **11**, p. 13, Feb. 2018.

[21] C. Arran, J. M. Cole, E. Gerstmayr, T. G. Blackburn, S. P. D. Mangles, and C. P. Ridgers, "Optimal Parameters for Radiation Reaction Experiments," *arXiv:1901.09015 [physics]* , Jan. 2019.

[22] T. D. Arber, K. Bennett, C. S. Brady, A. Lawrence-Douglas, M. G. Ramsay, N. J. Sircombe, P. Gillies, R. G. Evans, H. Schmitz, A. R. Bell, and C. P. Ridgers, "Contemporary particle-in-cell approach to laser-plasma modelling," *Plasma Phys. Control. Fusion* **57**, p. 113001, Nov. 2015.

[23] C. P. Ridgers, T. G. Blackburn, D. Del Sorbo, L. E. Bradley, C. Slade-Lowther, C. D. Baird, S. P. D. Mangles, P. McKenna, M. Marklund, C. D. Murphy, and A. G. R. Thomas, "Signatures of quantum effects on radiation reaction in laser–electron-beam collisions," *Journal of Plasma Physics* **83**, Oct. 2017.

[24] F. Niel, C. Riconda, F. Amiranoff, R. Duclous, and M. Grech, "From quantum to classical modeling of radiation reaction: A focus on stochasticity effects," *Physical Review E* **97**, Apr. 2018.